

In-Depth Characterization of the Major Leukocyte Cell Subsets in Human Peripheral Mononuclear Cells

Using the 45-color, full-spectrum Agilent NovoCyte Opteon spectral flow cytometer

Authors

Ming Lei,
Laurissa Ouaguia,
Garret Guenther,
Peifang Ye,
Nancy Li,
Agilent Technologies, Inc.

Abstract

Flow cytometry is a powerful technique for in-depth analysis of different immune cell subpopulations of immune cells to gather a comprehensive assessment of the immune system. Spectral flow cytometry has led to advancements in our capabilities to support more markers, greater flexibility, and better data resolution. In this application note, a 45-color spectral flow cytometry panel was designed for the Agilent NovoCyte Opteon spectral flow cytometer to analyze the distribution of immune cells in a peripheral blood mononuclear cell (PBMC) sample.

Introduction

An extraordinarily complex network of cells enables the immune system to recognize and remove dead and faulty cells while also defending the body from pathogens. As key drivers of the immune system, peripheral blood cells undergo activation, proliferation, and differentiation into various subsets characterized by a set of specific marker expressions and functions. Due to the simplicity and the noninvasiveness of its collection, peripheral blood has become a widely accessible source of peripheral blood mononuclear cells (PBMCs) which are vastly used in basic research, translational research, and clinical applications.¹⁻³ In healthy donors, PBMCs represent a heterogeneous cell population comprised of several immune cell types including but not limited to: lymphocytes (including T cells, B cells, natural killer (NK) cells, NKT cells, $\gamma\delta$ T cells, and innate lymphoid cells (ILCs)), monocytes, basophils, and dendritic cells (DC).^{1,3,4}

Most lymphocytes in peripheral blood are composed of CD3+ expressing T cells (45 to 70% PBMCs). Based on the expression of either an $\alpha\beta$ TCR or a $\gamma\delta$ TCR, two types of T cells can be distinguished.⁵ $\alpha\beta$ TCR expressing T cells can be further subdivided into conventional CD4+ T helpers (25 to 60%) and CD8+ T cytotoxic cells (5 to 30%). The CD4+T cells and CD8+T cell ratio to healthy donor PBMCs is around 2:1.^{3,6} CD4+T helpers are essential mediators of immune homeostasis and inflammation. Based on the expression profiles of specific surface markers/proteins, cytokines, chemokine receptors, and specific transcription factors, CD4+T cells can be further classified into Th1, Th2, Th17, Th9, Th22, follicular helper (Tfh) cell, recent thymic emigrants (RTE) and regulatory T cell (Treg) subsets.⁷⁻¹⁰ In addition, antigen-presenting cells, after presenting antigens to naive T cells, become activated and undergo differentiation into effector T cells and memory cells. Effector cells migrate to the site of infection and eliminate the pathogen. These effector cells are short-lived while the memory subsets formed have the potential for long-term survival.^{7,11} Conventional CD8+T cytotoxic cells are a key component of the adaptive immune system that fights intracellular infections and tumor cells. Similar to CD4+T cells, activation of naive CD8+ T cells induces a largely autonomous program of proliferation and differentiation, generating both effector and memory cells.⁷ Memory T cells are important drivers of immunity, as immunological memory is critical for long-term immunity and protection from infection.⁷ Despite the mutually exclusive CD4-CD8 paradigm, a small fraction of $\alpha\beta$ T cells are composed of unconventional T cells. These unconventional T cells are composed of double negative CD4-CD8-T cells^{5,12}

and double positive CD4+CD8+T cells.¹³ Unconventional T cells represent the least studied T cell subset and have been identified as key players in various conditions where they display either a cytotoxic function (chronic viral infections) or a regulatory role (malignancies). Similar to conventional T cells, unconventional T cells also express activation markers and exhibit memory-like features.¹³⁻¹⁵ CD3+T cells are also composed of regulatory T cells (Treg), which constitute 3 to 5% CD4+T cells in healthy PBMCs.¹⁶ Tregs have been identified using various approaches, including by the relative expression of CD3, CD4, CD25, and CD127 markers. Treg cells can be subdivided into natural Treg (nTreg), generated in the thymus, or peripheral inducible Treg (iTreg).^{17,18} Treg cells express many activation and memory features, are known to suppress immune responses to self-antigens, and play a role in peripheral tolerance maintenance.^{7,18} Another subset of peripheral CD3+T cells are the CD56+NKT cells (0.04 to 1.3% lymphocytes), capable of influencing the status of the innate and adaptive immune response.¹⁹ Based on the expression levels of CD16 and CD56 markers, NKT cells can be further divided into subsets, and similar to T cells, engagement of costimulatory molecules affects NKT cell activation and function.^{19,20}

Others unconventional T cells include $\gamma\delta$ T lymphocytes, which possess both innate and adaptive-like properties, building the bridge between innate and adaptive immunity.²¹ These abilities render $\gamma\delta$ T cells an attractive candidate for adoptive cell immunotherapy due to their unique biology. Based on the expression levels of specific factors and proteins, $\gamma\delta$ T cells can be subdivided into different subtypes.²²

Peripheral lymphocytes also include non-T cells such as B cells, NK cells, and ILCs.^{3,23} B cells are CD19+ expressing cells that secrete antibodies. As such, they are central elements in humoral immunity and protect against an almost unlimited variety of pathogens as part of the adaptive immune system. B cells represent around 15% PBMC and can mature and differentiate into plasmablasts, plasma cells, transitional B cells, memory B cells, follicular B cells, marginal zone B cells, B regulatory, and B-1 cells. Each B cell subset can be characterized based on the expression of a set of proteins and factors including CD27, IgM, IgG, IgD, and CD38.²⁴ PBMC composition also includes NK cells (approximately 10%) which are the cytotoxic natural killer cells representing critical components of the innate immune system by directly destroying pathogen infected cells. Based on the relative expression of the CD16 and CD56 markers, NK cells can be further divided into different subsets.^{3,20} PBMCs are also composed of ILCs lacking expression of lineage markers and

antigen-specific receptors. Despite these characteristics, ILCs generate of cytokines and secreted proteins leading to an improvement of the immune response in case of infection. Some ILCs have been shown to have many parallels with CD4+ T cell subsets. Therefore, ILCs can be further divided into specific subsets based on specific marker expression and cytokine production.^{25,26}

PBMCs also consist of DC cells (1 to 2%), which function as professional antigen-presenting cells with the unique property of inducing priming and differentiation of naive CD4+ and CD8+ T cells into helper T, cytotoxic effectors T, and memory T cells. Based on their ontology, localization, surface marker expression, cytokine production, antigen-processing, and presentation capacity, DC can be further divided into myeloid or conventional dendritic cells (CD11c/cDC2 and CD141/cDC1) and plasmacytoid dendritic cells (CD123/pDCs).^{27,28} PBMCs are also made of monocytes (10 to 20%) which represent a highly plastic innate immune cell type that displays significant heterogeneity in periphery. Distinct patterns of surface marker relative expression (CD16, CD14) have become accepted as a basis for distinguishing three monocyte subsets: nonclassical, intermediate, and classical monocytes.^{3,29} PBMC is also comprised of a small fraction of cells called basophils (< 1%) based on PBMC isolation methods. These basophils can be characterized based on relative expression of HLADR and CD123 markers.³⁰

There is a growing interest in deciphering the complex role of each blood immune cell subset to assess how they shape the immune response, impact cancer and disease progression, and affect drug efficacy. To overcome this challenge, there is a significant need for methodologies and instruments that provide high-throughput, in-depth analyses of the immune system at the single cell level and subset level. We developed a 45-color spectrum flow cytometry immunophenotyping panel to quantitate peripheral immune subset frequencies, protein expression, activation markers, exhaustion markers, and differentiation markers expressed on the major innate and adaptive immune cells types in healthy PBMC. Common surface markers expressed by each population were used to determine population frequencies and further characterization of each population was evaluated using markers associated with cell activation and proliferation (CD69, HLA-DR, CD38), cell exhaustion and senescence (PD1, CD223, CD57), cell differentiation (CCR7, CD27, CD28, CD45RA, CD45RO, CD127), and cell plasticity or migration potential (CXCR3, CCR6, CCR5, CXCR5). This in-depth analysis was made possible using the Agilent NovoCyte Opteon spectral flow cytometer.

Contrary to conventional cytometry, which is limited in obtaining the peak fluorophore emission from as many fluorescent parameters as there are detectors, spectral cytometry is set up with many detectors to capture the full fluorescence spectrum for every fluorophore across all laser lines. In doing so, spectral cytometry allows for more parameters per fluorochrome in a single experiment.^{1,31,32}

Experimental

Materials

Table 1 describes the materials used to prepare the 45-color samples.

Table 1. Reagents used.

Reagents	Part Number	Manufacturer
True-Stain Monocyte Blocker	426102	BioLegend
Brilliant Stain Buffer Plus	566385	BD
CellBlox Blocking Buffer	B001T02F01	Thermo Fisher Scientific
Phosphate Buffer Saline (PBS)	GNM-14190	Genom Biomedical Technology
Fetal Bovine Serum (FBS)	10091148	Thermo Fisher Scientific

Staining procedure

The following protocol describes the sample preparation.

Preparation of PBMCs

- Prewarm RPMI 1640 Complete Culture Medium at 37 °C for at least 30 minutes.
- Thaw the PBMC cryo tube (approximately 15×10^6 cells) in a 37 °C water bath until only a small piece of ice is left.
- Transfer the contents of the cryo tube to a 50 mL conical tube.
- Add 1 mL preheated RPMI 1640 Complete Culture Medium to the cryo tube and leave it for use in step g.
- Add 5 mL RPMI 1640 Complete Culture Medium drop by drop to the cells in a 50 mL tube. When adding, gently mix the 50 mL tube (hold the pipette in one hand and the 50 mL tube in the other, gently mix the tube while adding RPMI 1640 Complete Culture Medium).
- After adding the first batch of 5 mL RPMI 1640 Complete Culture Medium, the next 5 mL should be added slightly faster (a few drops each time).
- After adding 10 mL, transfer the contents of the cryo tube to the 50 mL tube.

- h. Add an additional volume of RPMI 1640 Complete Culture Medium to the 50 mL tube to reach 20 mL.
- i. Centrifuge at 400 g for 8 minutes.
- j. Carefully pour out the supernatant and do not disturb the pellet.
- k. Gently suspend the pellet in 2 mL of preheated RPMI 1640 Complete Culture Medium and complete to 20 mL.
- l. Repeat steps i and j.
- m. Suspend the cell sediment in a certain volume of RPMI 1640 Complete Culture Medium for later use.

Preparation of live/dead dyes and antibodies mixture

- a. Thaw Zombie NIR Live/Dead dye, transfer 0.25 μ L to a larger Eppendorf tube, and add 1000 μ L of 1x PBS (final dilution 1:4000), avoiding light until use.
- b. Mark four 1.5 mL Eppendorf tubes with: antibody mixture A, B, C, and D. Cells need to be stained in four steps for better staining.
- c. Add 10 μ L Brilliant Stain Buffer and 5 μ L True-Stain Monocyte Blocker to each antibody mixtures tube, add 5 μ L CellBlox Blocking Buffer to antibody mixture tube A only.
- d. Prepare the antibody mixture according to the antibody list (Table 2), add the antibodies from Group A to the tubes labeled with A, add the antibodies from Group B to the tubes labeled with B, and so on.
- e. Centrifuge all the mixture tubes at 16,000 g ~ 18,000 g for 5 minutes. When using the antibodies, aspirate the mixture from the top of the liquid, and do not touch the bottom of the tube. The antibody aggregates will be left in the bottom.

Table 2. Antibody staining groups, except CD45RO SBUV445 antibody.

	Specificity	Fluorochrome	Dosage (μ L)
Staining Group A			
1	CCR6	BV711	2.5
2	CCR5	BUV563	2.5
3	TCR γ δ	PerCP-eFluor 710	0.63
4	CXCR5	BV750	0.63
5	IgG	BV605	0.63
6	CXCR3	PE-Cy7	1.25
7	CD223 (LAG-3)	NovaFluor Blue 660/120S	1.25
8	CD69	StarBright Blue 765	1.25
9	CCR7	BV421	2.5
Staining Group B			
1	CD20	Spark YG 593	1.25
2	CD1c	Alexa Fluor 647	2.5
3	CD28	BV650	5
4	PD-1	BV785	5
5	CD159c	PE	10
Staining Group C			
1	CD127	Spark Red 718	1.25
2	CD2	PerCP-Cy5.5	2.5
3	CD337	PE-Dazzle 594	2.5
4	CD3	BV510	2.5
5	CD27	APC-H7	2.5
6	CD25	PE-Alexa Fluor 700	5
7	CD11c	eFluor 450	5
Staining Group D			
1	CD45RA	BUV395	0.32
2	IgD	BV480	0.32
3	CD4	CF594	0.32
4	CD14	Spark Blue 550	0.32
5	HLA-DR	PE-Fire 810	0.32
6	CD33	StarBright Blue 580	0.32
7	CD16	BUV496	0.63
8	CD57	FITC	0.63
9	CD24	PE-Alexa Fluor 610	0.63
10	CD95	PE-Cy5	0.63
11	CD38	APC-Fire 810	0.63
12	CD31	StarBright Blue 810	0.63
13	CD141	BB515	1.25
14	CD19	Spark NIR 685	1.25
15	CD8	BUV805	1.25
16	CD159a	APC	2
17	CD314	BUV615	2.5
18	CD56	BUV737	2.5
19	CD45	PerCP	2.5
20	IgM	BV570	2.5
21	CD39	BUV661	2.5
22	CD123	Super Bright 436	2.5

Staining

- a. Mark FACS tubes: unstained control tubes, single stained tubes, and multicolor tubes.
- b. Add 100 μL of cell suspension to each multicolor tube, approximately 3×10^6 cells, while adding 10 μL of cell suspension to each unstained control tube and single stained tubes, approximately 3×10^5 cells.
- c. Wash multicolor tubes and Live/Dead single staining tubes with PBS, while washing other single staining tubes and unstained control tubes with wash buffer (PBS + 2% FBS), 3 mL per tube.
- d. Centrifuge at 500 g for 5 minutes and carefully pour out the supernatant.
- e. Add 100 μL zombie NIR diluent to the multicolor tube and Live/Dead single staining tube; vortex well and place on ice in the dark for 30 minutes.
- f. At the same time, stain the other single staining tubes with the optimal antibody levels shown in Table 2 and place them on ice in the dark for 30 minutes. Add CellBlox Blocking Buffer for anti-CD223 NovaFluor Blue 660/120S single staining tube.
- g. After 30 minutes of incubation, wash the multicolor tubes, Live/Dead single staining tubes, and other single staining tubes with 3 mL wash buffer.
- h. Repeat step d.
- i. Add 200 μL wash buffer to Live/Dead single staining tubes, unstained control tubes, and other single staining tubes, vortex mix, and store on ice.
- j. Add anti-CD45RO SBUV445 to all multicolor tubes, vortex, and place on ice in dark for 30 minutes.
- k. No wash, add antibody mixture A to all multicolor tubes, vortex, and place on ice in the dark for 30 minutes, then room temperature (RT) for 20 minutes (which will make the staining of CCR and CXCR markers better).
- l. Wash all multicolor tubes once with 3 mL wash buffer.
- m. Repeat step d.
- n. Add antibody mixture B to all multicolor tubes, vortex, and place on ice in the dark for 40 minutes.
- o. Wash all multicolor tubes once with 3 mL wash buffer.
- p. Repeat step d.
- q. Add antibody mixture C to multicolor tubes, vortex, and place on ice in dark for 40 minutes.
- r. Wash all multicolor tubes once with 3 mL wash buffer.
- s. Repeat step d.
- t. Add antibody mixture D to multicolor tubes, vortex, and place on ice in the dark for 40 minutes.
- u. Wash all multicolor tubes twice with 3 mL wash buffer.
- v. Repeat step d.
- w. Add 300 μL wash buffer to the multicolor tubes, vortex, and store on ice.

Results and discussion

Antibody titrations

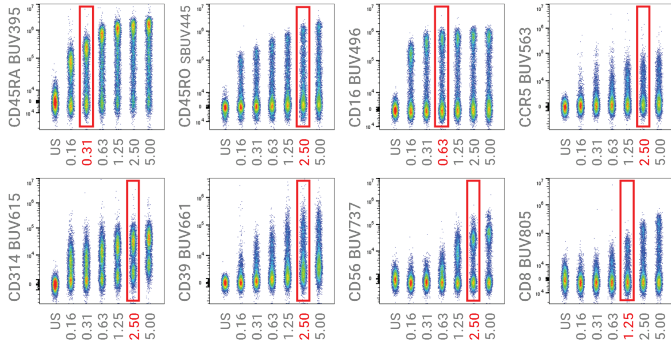
In this application note, all marker and fluorochrome combinations proposed in this 45-color panel (outlined in Table 3) are accessed by antibody titration analysis. The required volume of each antibody shown in Figure 1 is determined according to the stain index, which is calculated as follows: $(\text{MFI}(\text{positive}) - \text{MFI}(\text{negative})) / (2 * \text{SD}(\text{negative}))$, where MFI is mean fluorescence intensity. The optimal titration is chosen as the lowest concentration of antibody with a maximal or near-maximal stain index or lower spreading error.

The main objective of this panel design was to build off of a previously published 40-marker panel, OMIP-069. In addition to the OMIP-069 panel, we included five other markers: CD45RO, CD33, CD233 (LAG-3), CD69, and CD31. The entire panel of antibodies and fluorochromes is shown in Table 3. Due to the complex nature of staining with such a large panel induced by steric hindrances, four staining groups were identified to optimize the antibody-antigen binding and incubated with the sample in a sequential pattern (Table 2).

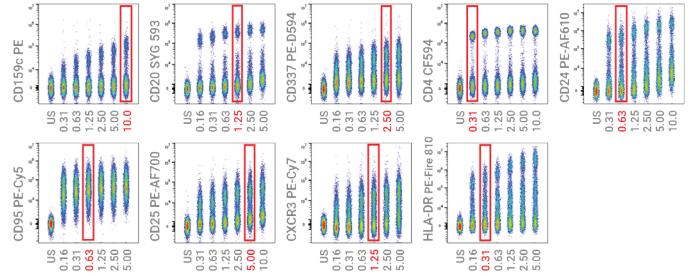
Table 3. Antibody information.

	Marker	Fluorochrome	Clone	Manufacturer	Part Number
1	CD45RA	BUV395	5H9	BD Biosciences	740315
2	CD45RO	StarBright UltraViolet 445	UCHL1	Bio-RAD	MCA461SBUV445
3	CD16	BUV496	3G8	BD Biosciences	612945
4	CCR5(CD195)	BUV563	2D7/CCR5	BD Biosciences	741401
5	CD314(NKG2D)	BUV615	1D11	BD Biosciences	751232
6	CD39	BUV661	TU66	BD Biosciences	749967
7	CD56	BUV737	NCAM16.2	BD Biosciences	612766
8	CD8	BUV805	SK1	BD Biosciences	612889
9	CCR7(CD197)	BV421	G043H7	BioLegend	353208
10	CD123	Super Bright 436	6H6	Thermo Fisher Scientific	62-1239-42
11	CD11c	eFluor 450	3.9	Thermo Fisher Scientific	48-0116-42
12	IgD	BV480	IA6-2	BD Biosciences	566187
13	CD3	BV510	SK7	BioLegend	344827
14	IgM	BV570	MHM-88	BioLegend	314517
15	IgG	BV605	G18-145	BD Biosciences	563246
16	CD28	BV650	CD28.2	BioLegend	302945
17	CCR6(CD196)	BV711	G034E3	BioLegend	353435
18	CXCR5(CD185)	BV750	RF8B2	BD Biosciences	747111
19	PD-1(CD279)	BV785	EH12.2H7	BioLegend	329929
20	CD141	BB515	1A4	BD Biosciences	565084
21	CD57	FITC	NK-1	BD Biosciences	555619
22	CD14	Spark Blue 550	63D3	BioLegend	367148
23	CD33	StarBright Blue 580	WM53	Bio-RAD	MCA1271SBB580
24	CD223(LAG-3)	NovaFluor Blue 660/120S	3DS223H	Thermo Fisher Scientific	H048T02B08
25	CD45	PerCP	HI30	Agilent Technologies	8931017
26	CD2	PerCP-Cy5.5	TS1/8	BioLegend	309225
27	TCRγδ	PerCP-eFluor 710	B1.1	Thermo Fisher Scientific	46-9959-41
28	CD69	StarBright Blue 765	FN50	Bio-RAD	MCA2806SBB765
29	CD31	StarBright Blue 810	WM59	Bio-RAD	MCA1738SBB810
30	CD159c(NKG2C)	PE	134591	R&D Systems	FAB138P-100
31	CD20	Spark YG 593	2H7	BioLegend	302367
32	CD337(Nkp30)	PE-Dazzle 594	P30-15	BioLegend	325231
33	CD4	CF594	C4/206	Biotium	#BNC940206-500
34	CD24	PE-Alexa Fluor 610	SN3	Thermo Fisher Scientific	MHCD2422
35	CD95(FAS)	PE-Cy5	DX2	BioLegend	305610
36	CD25	PE-Alexa Fluor 700	CD25-3G10	Thermo Fisher Scientific	MHCD2524
37	CXCR3(CD183)	PE-Cy7	G025H7	BioLegend	353720
38	HLA-DR	PE-Fire 810	L243	BioLegend	307683
39	CD159a(NKG2A)	APC	REA110	Miltenyi	130-113-563
40	CD1c	Alexa Fluor 647	L161	BioLegend	331510
41	CD19	Spark NIR 685	HIB19	BioLegend	302269
42	CD127	Spark Red 718	A019D5	BioLegend	351376
43	Viability	Zombie NIR	N/A	BioLegend	423105
44	CD27	APC-H7	M-T271	BD Biosciences	560223
45	CD38	APC-Fire 810	HB-7	BioLegend	356643

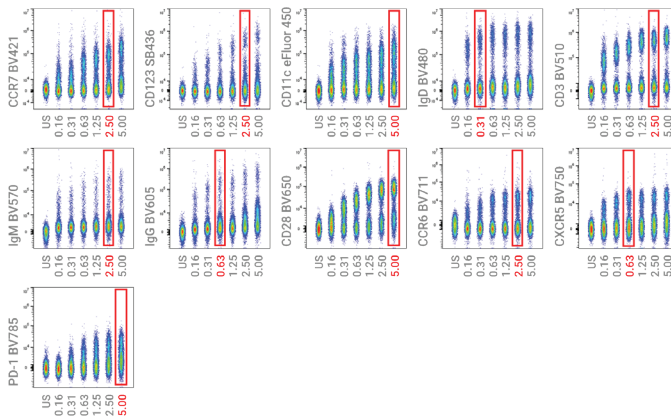
A. UV laser (349 nm)



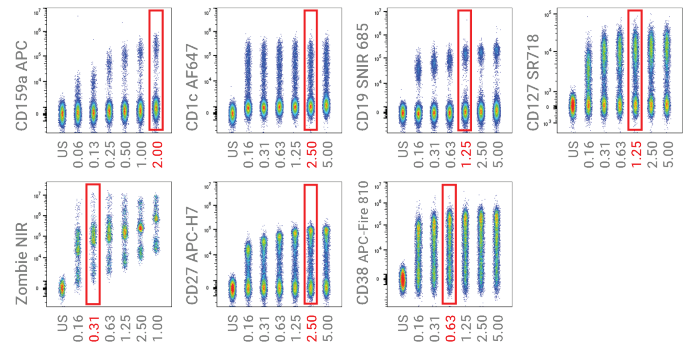
D. Yellow laser (561 nm)



B. Violet laser (405 nm)



E. Red laser (637 nm)



C. Blue laser (488 nm)

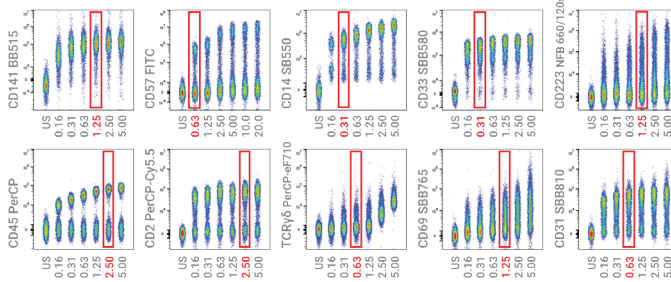
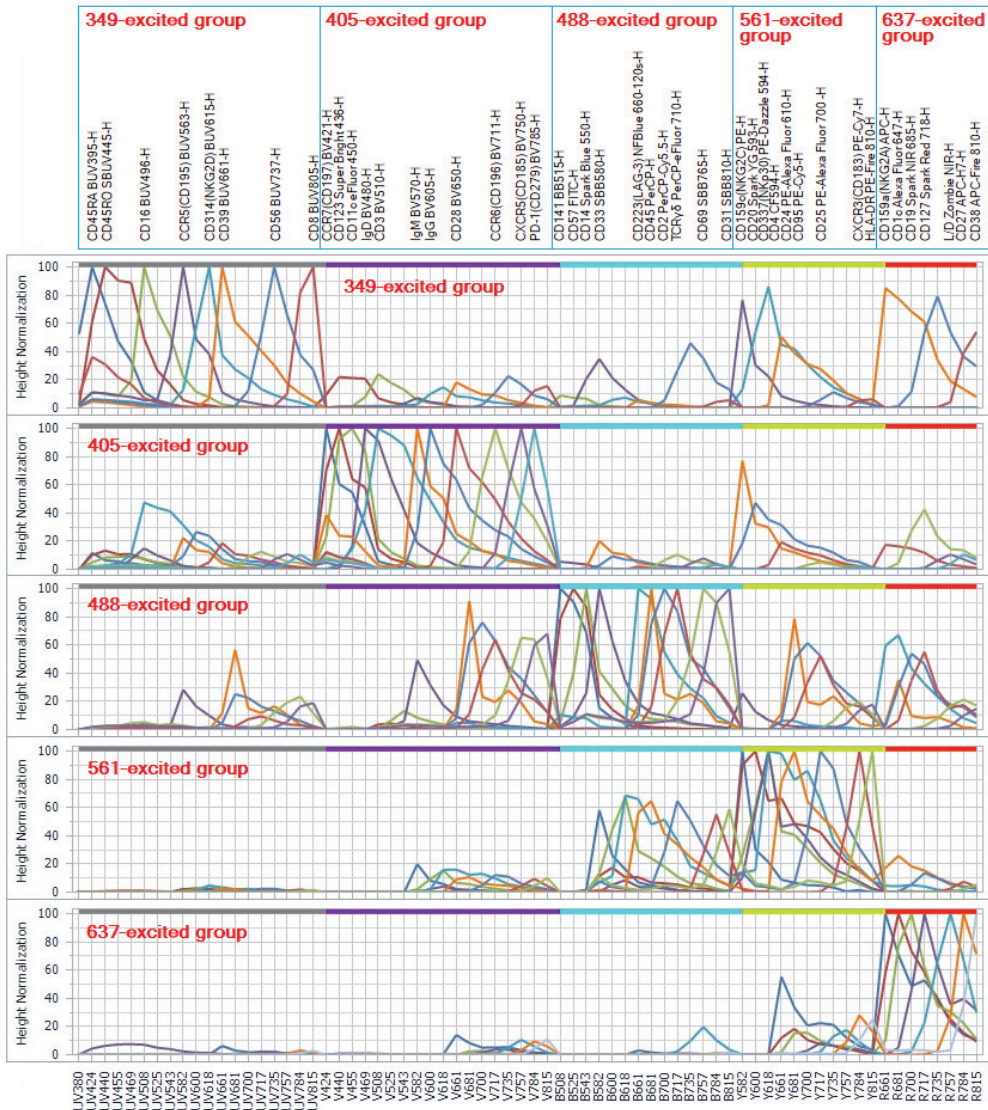


Figure 1. Antibody titrations for the 45-color panel. All antibodies are titrated over six concentrations with a starting concentration ranging from 1 to 20 μL per 100 μL staining volume using the cryopreserved PBMC separated from leukopak collected from healthy individuals. All six dilutions are shown on the same plot with the X-axis demonstrated the dilution series. The red square highlights the final selected titer used for the panel. The optimal titer is chosen based on stain index (the lowest concentration of antibody with a maximal or near-maximal stain index or lower spreading error) and is indicated by the red box. All titration data were unmixed by the Agilent NovoExpress 2.0.0 software; debris and doublets were excluded, and files are concatenated using FlowJo v10.10.0. (A) 349 nm laser excited fluorochromes, (B) 405 nm laser excited fluorochromes, (C) 488 nm laser excited fluorochromes, (D) 561 nm laser excited fluorochromes, (E) 637 nm laser excited fluorochromes. The stain index was calculated as follows: $(\text{MFI}(\text{positive}) - \text{MFI}(\text{negative})) / (2 * \text{SD}(\text{negative}))$, where MFI is mean fluorescence intensity.

Reference spectra controls were run for each marker used, including two populations for autofluorescence (AF) subtraction as visualized in Figure 2.

A. Spectral signatures of 45 fluorochromes



B. Spectral signatures of two autofluorescence

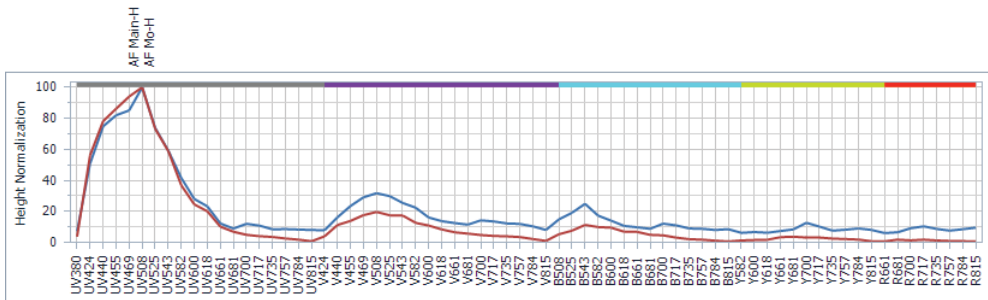


Figure 2. Spectral signatures (45 + 2 AF) used for unmixing the 45-color panel data. Single stained controls were acquired on the Agilent NovoCyte Opteon spectral flow cytometer at the default gain settings. Fluorochrome spectral signatures (normalized emission spectra) are shown as spectral plots grouped by primary laser and autofluorescence. (A) 45 fluorochromes; (B) Two autofluorescence signatures.

The distribution of immune cell types and subtypes were identified based on their marker expression, and hierarchical gating was used to specify each, as outlined in Figure 5.

Unmixed data categorized with different cell types is shown in Figure 5, highlighting the complexity and depth in which we are able to characterize many subtypes in this panel.

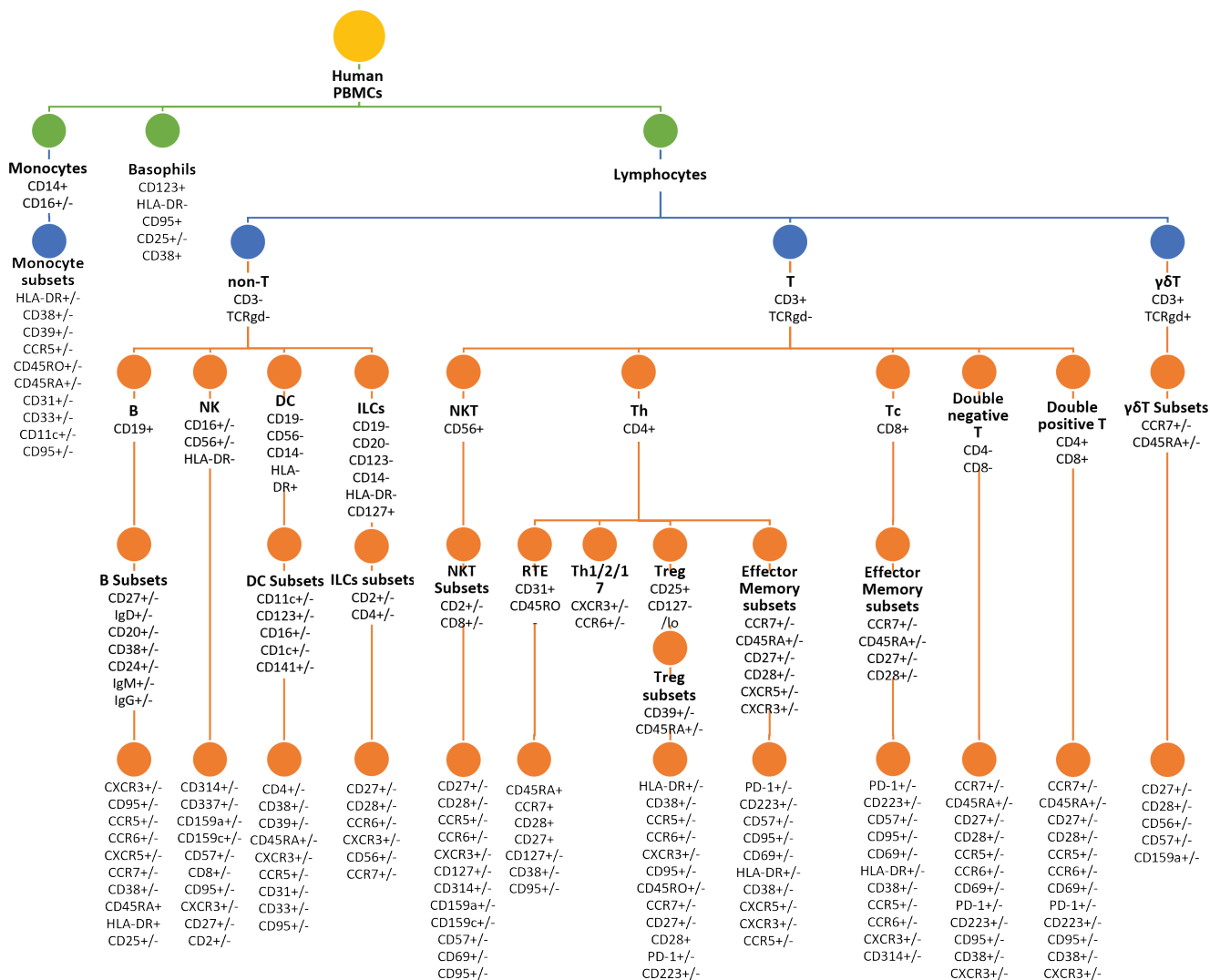


Figure 5. Schematic overview of all the identified cell subsets.

Manual gating strategy used to identify the main immune cell subsets

PBMCs are processed following protocols describing the sequencing staining procedure, as shown in Figure 6. After platelets, debris, doublets and dead cells were excluded, within the live CD45+ population, basophils (1) were delineated as CD45+CD123+HLA-DR-. Lymphocytes and monocytes (2) were gated based on FSC-H/BSSC-H properties. Monocytes (3) were then classified by CD14 and CD16 expression as non-classical (CD14-CD16+), intermediate (CD14+CD16+/low), and classical (CD14+CD16-). From the lymphocyte gate (2), the following populations were identified: CD3-TCR $\gamma\delta$ -, CD3+TCR $\gamma\delta$ +, and CD3+TCR $\gamma\delta$ - (4). The CD3+TCR $\gamma\delta$ + population (5) was characterized based on CD45RA and CCR7 expression. The CD3+TCR $\gamma\delta$ - population was divided in CD3+CD56+ (NKT-like) and CD3+CD56- subsets (6). The inclusion of CD2 and CD8 enables further classification of the NKT-like cells, CD69 and CD57 were used to detect the early activation and cytotoxicity of NKT-like cells (7). CD4+, CD8+, CD4+CD8+, and CD4-CD8- T cells were identified from the CD3+CD56- gate (8). Treg cells were identified from the CD4+ population using CD127 and CD25 expression (CD127^{lo}/-CD25^{hi}), and CD39 and CD45RA were used to further classify these cells (9). CCR7, CD45RA, CD27, and CD28 allowed for further classification of memory/effector CD4 and CD8 T cell subsets, CXCR3 and CCR6 allowed for further classification of Th populations, CD45RO and CD31 were used to detect RTE cells within CD4 T cells, PD-1 and CD223 were used to

detect the exhaustion status of CD4 and CD8 T cells (10, 11). CD19+ and/or CD20+ cells (B cells) were gated out of the CD3-TCR $\gamma\delta$ - population (12). CD19+CD20+/- cells were further gated as IgD+CD27-, IgD+CD27+, or IgD-CD27+/-; the IgD-CD27+/- subset was divided into plasmablasts or IgD-memory B cells based on CD20 expression, and IgG and IgM expression were assessed within the IgD- memory B cells; the IgD+CD27- population was further divided into transitional B cells; the IgD+CD27+ population was further divided into MZ and IgD- Memory only B cells (13). NK cells were defined as CD3-TCR $\gamma\delta$ -HLA-DR- and classified as early NK (CD56+CD16-), mature NK (CD56+CD16+), and terminal NK (CD56-CD16+) cells (14). Dendritic cells (DCs, 15) were identified first by gating on CD3-CD19-CD56-CD14-HLA-DR+ and from there CD123+ (pDCs) and CD11c+ DCs were identified. CD11c+ DCs were further divided into CD16- and CD16+. CD1c and CD141 were then used to further classify the CD11c+CD16- and CD11c+CD16+ DCs. Finally, innate lymphoid cells (ILCs, 16) were identified as CD3-CD19-CD20-CD14-CD123-CD127+ and further classified based on CD2 and CD4 expression. All data presented is derived from frozen PBMCs of one healthy donor.

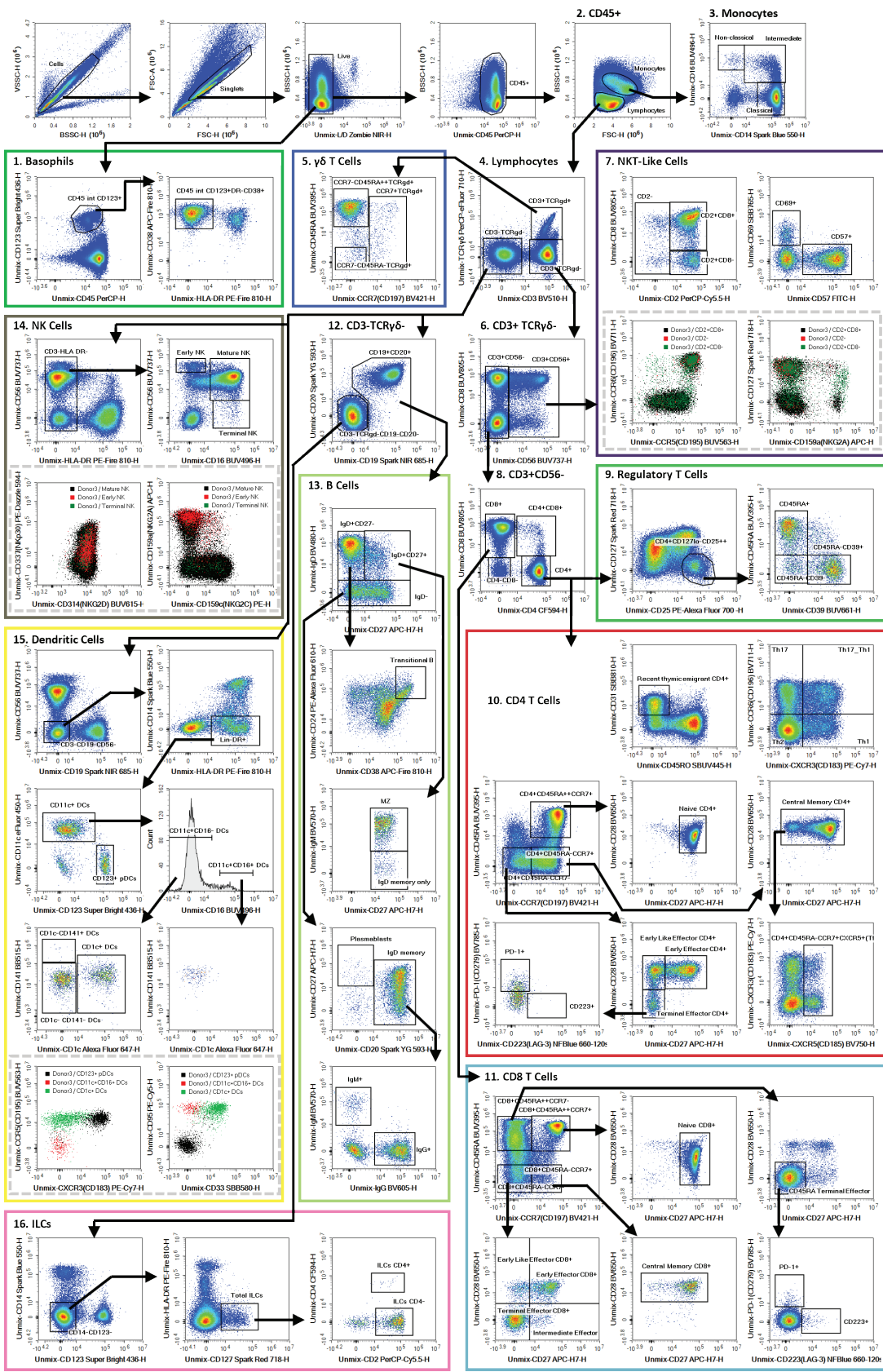


Figure 6. The cell types characterized in a normal human PBMC sample after removing platelets, debris, doublets, and dead cells are as follows: monocytes, basophils, natural killer cells, dendritic cells, innate lymphoid cells, B-, T-, NKT-like, Treg, and TCR $\gamma\delta$ lymphocytes. Other markers were included to assess differentiation, exhaustion, or activation status were also included.

Conclusion

Spectral flow cytometry offers the ability to analyze more markers simultaneously with improved data resolution and panel design flexibility. Used in this study, the Agilent NovoCyte Opteon offers these benefits, along with the easy-to-use Agilent NovoExpress data acquisition and analysis software. With five lasers (UV, V, B, Y, R) and 73 total photodetectors, the NovoCyte Opteon is able to meet the requirements of increasingly sophisticated experimental panels and enable an efficient workflow to uncover answers that may not be met with conventional flow cytometry.

References

1. Sen, P.; Kemppainen, E.; Oresic, M. Perspectives on Systems Modeling of Human Peripheral Blood Mononuclear Cells. *Front Mol Biosci* **2017**, *4*:96.
2. Corkum, C.P.; Ings, D.P.; Burgess, C.; Karwowska, S.; Kroll, W.; Michalak, T.I. Immune Cell Subsets and Their Gene Expression Profiles From Human PBMC Isolated by Vacutainer Cell Preparation Tube (CPT) and Standard Density Gradient. *BMC Immunol* **2015**, *16*:48.
3. Kleiveland, C.R. Peripheral Blood Mononuclear Cells. In: The Impact of Food Bioactives on Health: In Vitro and Ex Vivo Models. Edited by Verhoeckx K, Coter P, Lopez-Exposito I, Kleiveland C, Lea T, Mackie A, Requena T, Swiatecka D, Wichers H. *Cham (CH)*; **2015**, 161–167.
4. Lozano-Ojalvo, D.; Lopez-Fandino, R.; Lopez-Exposito, I. PBMC-Derived T Cells. In: The Impact of Food Bioactives on Health: In Vitro and Ex Vivo Models. Edited by Verhoeckx K, Coter P, Lopez-Exposito I, Kleiveland C, Lea T, Mackie A, Requena T, Swiatecka D, Wichers H. *Cham (CH)*; **2015**, 169–180.
5. Morath, A.; Schamel, W.W. Alphabeta and Gammadelta T Cell Receptors: Similar but Different. *J Leukoc Biol* **2020**, *107*(6):1045–1055.
6. McBride, J.A.; Striker, R. Imbalance in the Game of T Cells: What Can the CD4/CD8 T-Cell Ratio Tell Us About HIV and Health? *PLoS Pathog* **2017**, *13*(11):e1006624.
7. Golubovskaya, V.; Wu, L. Different Subsets of T Cells, Memory, Effector Functions, and CAR-T Immunotherapy. *Cancers (Basel)* **2016**, *8*(3).
8. Sakaguchi, S.; Yamaguchi, T.; Nomura, T.; Ono, M. Regulatory T Cells and Immune Tolerance. *Cell* **2008**, *133*(5):775–787.
9. Raphael, I.; Nalawade, S.; Eagar, T.N.; Forsthuber, T.G. T Cell Subsets and Their Signature Cytokines in Autoimmune and Inflammatory Diseases. *Cytokine* **2015**, *74*(1):5-17.
10. Pido-Lopez, J.; Imami, N.; Aspinall, R. Both Age and Gender Affect Thymic Output: More Recent Thymic Migrants in Females Than Males as They Age. *Clin Exp Immunol* **2001**, *125*(3):409–413.
11. Gatinoni, L.; Speiser, D.E.; Lichterfeld, M.; Bonini, C. T Memory Stem Cells in Health and Disease. *Nat Med* **2017**, *23*(1):18–27.
12. Li, H.; Tsokos, G.C. Double-Negative T Cells in Autoimmune Diseases. *Curr Opin Rheumatol* **2021**, *33*(2):163–172.
13. Desfrancois, J.; Moreau-Aubry, A.; Vignard, V.; Godet, Y.; Khammari, A.; Dreno, B.; Jotereau, F.; Gervois, N. Double Positive CD4CD8 Alphabeta T Cells: A New Tumor-Reactive Population in Human Melanomas. *PLoS One* **2010**, *5*(1):e8437.
14. Gonzalez-Mancera, M.S.; Bolanos, N.I.; Salamanca, M.; Orjuela, G.A.; Rodriguez, A.N.; Gonzalez, J.M. Percentages of CD4+CD8+ Double-Positive T Lymphocytes in the Peripheral Blood of Adults from a Blood Bank in Bogota, Colombia. *Turk J Haematol* **2020**, *37*(1):36–41.
15. Kitchen, S.G.; Whitmire, J.K.; Jones, N.R.; Galic, Z.; Kitchen, C.M.; Ahmed, R.; Zack, J.A. The CD4 Molecule on CD8+ T Lymphocytes Directly Enhances the Immune Response to Viral and Cellular Antigens. *Proc Natl Acad Sci U S A* **2005**, *102*(10):3794–3799.
16. Santegoets, S.J.; Dijkgraaf, E.M.; Bataglia, A.; Beckhove, P.; Briten, C.M.; Gallimore, A.; Godkin, A.; Goutefangeas, C.; de Gruijl, T.D.; Koenen, H.J.; et al Monitoring Regulatory T Cells in Clinical Samples: Consensus on an Essential Marker Set and Gating Strategy for Regulatory T Cell Analysis by Flow Cytometry. *Cancer Immunol Immunother* **2015**, *64*(10):1271–1286.
17. Ouaguia, L.; Morales, O.; Mrizak, D.; Ghazal, K.; Boleslawski, E.; Auriault, C.; Pancre, V.; De Launoit, Y.; Conti, F.; Delhem, N. Overexpression of Regulatory T Cells Type 1 (Tr1) Specific Markers in a Patient with HCV-Induced Hepatocellular Carcinoma. *ISRN Hepatol* **2013**, 2013:928485. <https://www.ncbi.nlm.nih.gov/pmc/articles/PMC4890904/>
18. Ouaguia, L.; Mrizak, D.; Renaud, S.; Morales, O.; Delhem, N. Control of the Inflammatory Response Mechanisms Mediated by Natural and Induced Regulatory T-Cells in HCV-, HTLV-1-, and EBV-Associated Cancers. *Mediators Inflamm* **2014**, 2014:564296.
19. Khan, M.A.; Khan, A. Role of NKT Cells during Viral Infection and the Development of NKT Cell-Based Nanovaccines. *Vaccines (Basel)* **2021**, *9*(9).

20. Poli, A.; Michel, T.; Theresine, M.; Andres, E.; Hentges, F.; Zimmer, J. CD56 Bright Natural Killer (NK) Cells: an Important NK Cell Subset. *Immunology* **2009**, *126*(4):458–465.
21. Melandri, D.; Zlatareva, I.; Chaleil, R.A.G.; Dart, R.J.; Chancellor, A.; Nussbaumer, O.; Polyakova, O.; Roberts, N.A.; Wesch, D.; Kabelitz, D.; et al. The $\gamma\delta$ TCR Combines Innate Immunity with Adaptive Immunity by Utilizing Spatially Distinct Regions for Agonist Selection and Antigen Responsiveness. *Nat Immunol* **2018**, *19*(12):1352–1365. <https://www.nature.com/articles/s41590-018-0253-5>
22. Yazdanifar, M.; Barbarito, G.; Bertaina, A.; Airoidi, I. Gammadelta T Cells: The Ideal Tool for Cancer Immunotherapy. *Cells* **2020**, *9*(5).
23. Lunt, S.Y.; Vander Heiden, M.G. Aerobic Glycolysis: Meeting the Metabolic Requirements of Cell Proliferation. *Annu Rev Cell Dev Biol* **2011**, *27*:441–464.
24. Pieper, K.; Grimbacher, B.; Eibel, H. B-Cell Biology and Development. *J Allergy Clin Immunol* **2013**, *131*(4): 959–971.
25. Jacquelot, N.; Seillet, C.; Vivier, E.; Belz, G.T. Innate Lymphoid Cells and Cancer. *Nat Immunol* **2022**, *23*(3):371–379.
26. Chung, D.C.; Jacquelot, N.; Ghaedi, M.; Warner, K.; Ohashi, P.S. Innate Lymphoid Cells: Role in Immune Regulation and Cancer. *Cancers (Basel)* **2022**, *14*(9).
27. Sosa Cuevas, E.; Ouaguia, L.; Mouret, S.; Charles, J.; De Fraipont, F.; Manches, O.; Valladeau-Guilemond, J.; Bendriss-Vermare, N.; Chaperot, L.; Aspod, C. BDCA1(+) cDC2s, BDCA2(+) pDCs and BDCA3(+) cDC1s Reveal Distinct Pathophysiologic Features and Impact on Clinical Outcomes in Melanoma Patients. *Clin Transl Immunology* **2020**, *9*(11):e1190.
28. Ouaguia, L.; Leroy, V.; Dufeu-Duchesne, T.; Durantel, D.; Decaens, T.; Hubert, M.; Valladeau-Guilemond, J.; Bendriss-Vermare, N.; Chaperot, L.; Aspod, C. Circulating and Hepatic BDCA1+, BDCA2+, and BDCA3+ Dendritic Cells Are Differentially Subverted in Patients With Chronic HBV Infection. *Front Immunol* **2019**, *10*:112.
29. Cormican, S.; Griffin, M.D. Human Monocyte Subset Distinctions and Function: Insights From Gene Expression Analysis. *Front Immunol* **2020**, *11*:1070.
30. Voskamp, A.L.; Prickett, S.R.; Mackay, F.; Rolland, J.M.; O'Hehir, R.E. MHC Class II Expression in Human Basophils: Induction and Lack of Functional Significance. *PLoS One* **2013**, *8*(12):e81777.
31. Park, L.M.; Lannigan, J.; Jaimes, M.C. OMIP-069: Forty-Color Full Spectrum Flow Cytometry Panel for Deep Immunophenotyping of Major Cell Subsets in Human Peripheral Blood. *Cytometry A* **2020**, *97*(10):1044-1051.
32. Shevchenko, Y.; Lurje, I.; Tacke, F.; Hammerich, L. Fluorochrome-Dependent Specific Changes in Spectral Profiles Using Different Compensation Beads or Primary Cells in Full Spectrum Cytometry. *Cytometry A* **2024**.

www.agilent.com/lifesciences/cellanalysis

For Research Use Only. Not for use in diagnostic procedures.
RA45406.3860069444

This information is subject to change without notice.

© Agilent Technologies, Inc. 2024
Published in the USA, May 30, 2024
5994-7397EN

